ELSEVIER

Physics of the Earth and Planetary Interiors 104 (1997) 247–256

PHYSICS OF THE EARTH AND PLANETARY INTERIORS

Crustal heterogeneity as inferred from seismic coda wave decomposition by small-aperture array observation

Yasuto Kuwahara [a,*], Hisao Ito [a], Hitoshi Kawakatsu [b], Takao Ohminato [a], Tsutomu Kiguchi [a]

[a] *Geological Survey of Japan, 1-1-3 Higashi, Tsukuba, Ibaraki 305, Japan*
[b] *Earthquake Research Institute, 1-1-1 Yayoi, Bunkyou-ku, Tokyo 113, Japan*

Received 5 July 1996; received in revised form 2 January 1997; accepted 10 January 1997

Abstract

Seismic coda waves have complex waveforms and are considered to be caused by 3-dimensional structural heterogeneities. We carried out 3-component small-aperture array observations of seismic coda waves from natural earthquakes in Tsukuba, central Japan, to decompose complex coda waveforms and to clarify the nature of crustal heterogeneity. Epicentral distances in the present study are less than 200 km. The observational results are summarized as follows: 1) The remarkable feature of the coda from natural earthquakes is the difference between the P-coda and the S-coda especially in the vertical component. The P-coda consists mainly of coherent P-wave phases which have almost the same slowness vector as the initial P-wave motion, whereas the S-coda is decomposed into incoherent phases with random propagation directions. 2) Coherency of waveforms among the array sensors of the vertical component rapidly becomes low from the high value of coherency of the direct S-wave. 3) In the two horizontal components, radial and transverse ones, both the P- and S-coda are decomposed into incoherent random phases. 4) Coherency in the early S-coda of the horizontal components gradually becomes low compared to the vertical component. These features indicate that S to P converted waves at horizontal boundaries of the structure are dominant in the P-coda of the vertical component, while the P-coda of the horizontal components and the S-coda consist of scattered waves from the lateral heterogeneity. This interpretation leads to a model of crustal heterogeneity in which the degree of the lateral heterogeneity is smaller than the degree of vertical heterogeneity of layered structures. © 1997 Elsevier Science B.V.

Keywords: Seismic coda waves; Earthquakes; Japan; Crustal heterogeneity

1. Introduction

Seismic coda waves have been interpreted as scattered waves from randomly distributed heterogeneities in the Earth. Aki (1969) and Aki and Chouet (1975) presented models to estimate a seismic attenuation factor Q of the coda wave. The factor Q, which is commonly referred to as Q_{coda}, is almost equal to S-wave Q. Sato (1984) theoretically analyzed in detail a uniformly random heterogeneous structure to obtain envelopes of S-coda. Thus, the analysis of the S-coda envelope has been a powerful tool to estimate Q structures around a seismic observation site.

Lateral heterogeneity models are commonly pre-

* Corresponding author. Tel.: +81-298-54-3682; fax: +81-298-54-3533; e-mail: g8702@gsj.go.jp

PII S0031-9201(97)00057-5

sented in order to explain the coda excitation. On the other hand, layered structure models are also introduced in many places based on seismic reflection exploration (e.g. Fuchs et al., 1987) or coda excitation (Campillo and Paul, 1992). Both classes of models seem to be able to explain the coda excitation observed by a single seismic station. However, these two models are apparently inconsistent. In order to verify the model, it is necessary to determine propagation directions of wave energy composing coda waves by array techniques.

By using array techniques in contrast to the coda envelope analysis, we can determine the slowness vector of wave energy composing the coda wave. From this point of view, a number of studies have been performed on regional array data, such as the NORESS array in Norway (Jepsen and Kennett, 1990; Dainty and Toksoz, 1990) and the WRA (Warramunga) array in Australia (Kennett, 1987; King et al., 1973) and on temporal small-aperture array data (Aki, 1959; Kuwahara et al., 1990; Wagner and Owens, 1993). Some of these studies demonstrate that P-coda is composed of wave energy propagating from an epicentral direction and that the propagation directions of the S-coda are random. Kuwahara et al. (1990) discovered continuous arrival of wave energy in the P-coda from the epicentral direction in the Oshima volcano for an intermediate-depth earthquake. They explained the P-coda as being the trapped wave in a low velocity zone of subducting oceanic crust. This explanation is based on the particular position of the Oshima volcano relative to the subducting Philippine Sea plate. However, the same characteristics of P-coda are also reported in other areas (Jepsen and Kennett, 1990; Wagner and Owens, 1993). Although these authors did not give a clear explanation of this phenomenon, the P-coda reported by them could not seem to be explained by such a trapped wave as in the model by Kuwahara et al. (1990).

We have conducted a small-aperture array observation in the Tsukuba area of the Kanto basin, central Japan. Tsukuba has a different tectonic setting from Oshima volcano, so trapped waves are not expected. We report the results of array analysis of coda waves and propose a model of structural heterogeneity which explains the excitation of P- and S-codas.

2. Small-aperture array observation and data analysis

The array observation of natural earthquakes was performed in Tsukuba, central Japan from July, 1990 to October, 1992. Tsukuba is positioned in the northeastern part of the Kanto basin. Fig. 1 shows the observation site and the hypocenter distribution of the events which were triggered during the observation period. The most earthquakes triggered are along the Philippine Sea (PHS) plate subducting northwestward beneath the Kanto district and/or the Pacific (PAC) plate subducting westward beneath the Philippine Sea plate. The PHS and PAC plate boundaries are schematically illustrated in the east–west cross section along the latitude 36°N according to Ishida (1992).

Fig. 2 shows the configuration of the array. The array was placed in a tunnel for building maintenance for high power electric cables, water pipes and so on. The depth of the tunnel floor is about 9 m below the surface. The array consisted of 7 ~ 13 seismometers with two 200-meter arms; one extending NE–SW and the other perpendicular to that. The sensor spacing was about 50 m. The propagation

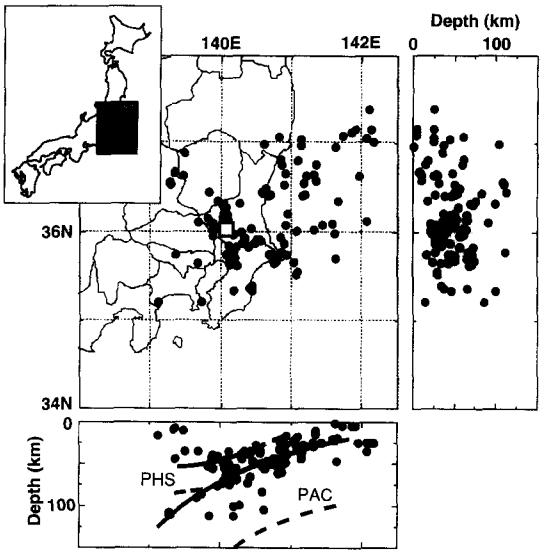

Fig. 1. Array observation site (open square) and hypocenter distribution (closed circles). The Philippine Sea (PHS) and Pacific (PAC) plate boundaries are schematically illustrated in the east–west cross section along the latitude 36°N according to Ishida (1992).

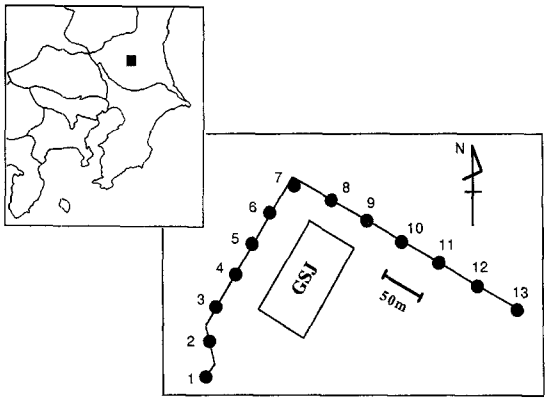

Fig. 2. Array configuration. The seismometers are placed in a tunnel for building maintenance.

directions of wave energy with a wavelength larger than about 100 m (twice of the sensor spacing) can be determined without the spacial aliasing for this array configuration. The first stage of observation was performed with 13 vertical component seismometers and a horizontal one. The second stage of observation was performed with 7 three-component seismometers. The sensors were Mark Products 2 Hz L-22 short-period seismometers with a damping factor of 0.7. The data were event triggered and recorded with 16-bit analog to digital converter at a sampling period of 0.003 s.

It is noted that the noise level is rather high at the observation site because the site is in the tunnel for building maintenance. The noise level is about 1 mkine (10^{-5} m/s). However, the seismic activity is very high around Tsukuba so that more than 70 felt earthquakes have occurred in a year in average. We could obtain enough data with sufficient S/N ratio in spite of the bad noise conditions.

An example of the three-component array records is shown in Fig. 3. The hypocenter of this event is located at 35.745°N, 140.932°E, and the depth of 16.2 km. The observational coordinate system, Z,

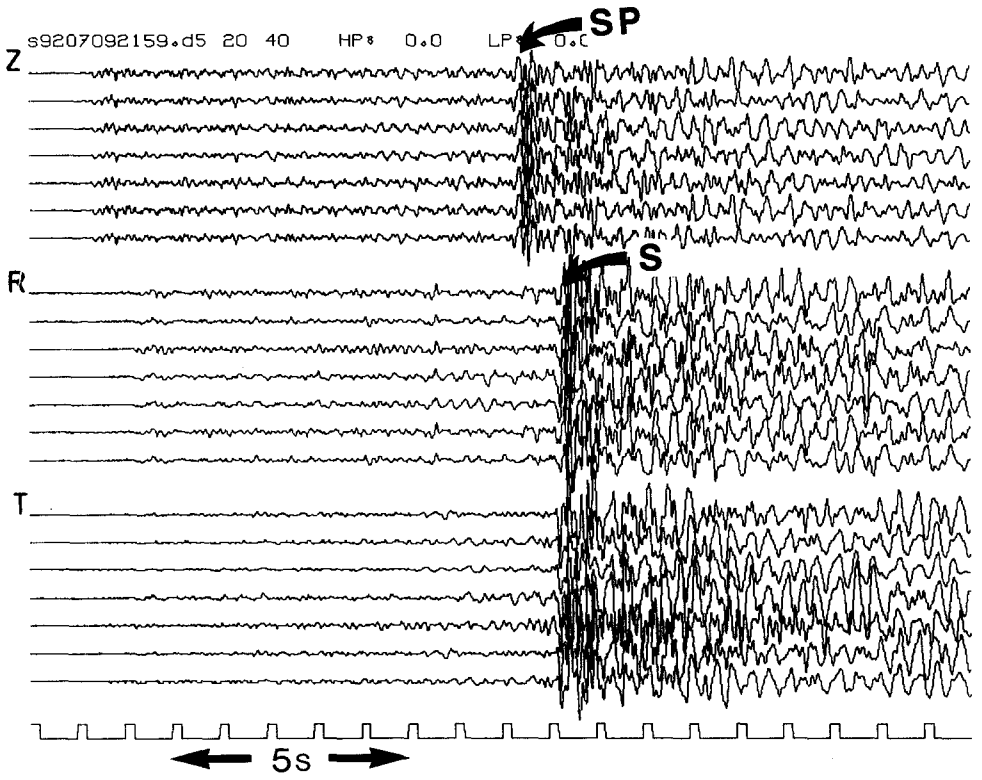

Fig. 3. An example of three-component array records. The velocity components are Z, radial (R), and transverse (T). The hypocenter of this event is located at 35.745°N, 140.932°E, and the depth of 16.2 km.

Table 1
Velocity structure of the shallow part of Tsukuba (from Kinoshita, 1990)

	Vp (km/s)	Vs (km/s)	ρ (g/cm^3)	H (m)
Layer 1	2.0	0.53	2.0	410
Layer 2	4.5	2.5	2.5	–

NS, EW was transformed into the system, Z, radial (R) and transverse (T) based on the hypocenter location. It can be qualitatively found that the waveforms of the Z-component in the P-coda are coherent among the array sensors although those in the S-coda do not remain coherent. The radial and transverse components are coherent only for the direct S-wave and relatively incoherent in both the P- and S-coda.

It should be noted that the dominant S–P converted phases in the Z-component are seen at about 0.9 s before the direct S-wave arrivals in the R- and T-components. This converted phase is due to the boundary between the sediment and the basement rock. Table 1 shows the average velocity structure of the shallow part from the borehole logging data of Kinoshita (1990) at the site 8 km northwest from the array observation point. If we assume the values of P- and S-wave velocities in the sedimentary layer beneath the array observation site are the same as in Table 1, the thickness of the sedimentary layer is about 700 m from the time delay between the S–P converted phase and the direct S-wave arrival. This value of 700 m is consistent with the estimation of the basement structure based on some borehole data around this region.

We have used a semblance technique to measure a multichannel coherency (Neidell and Taner, 1971). The resolution and efficiency of this technique are quite good as demonstrated by Kuwahara et al. (1990). The semblance can be regarded as the ratio of the energy of the stack with a certain slowness vector within a certain time window to the sum of

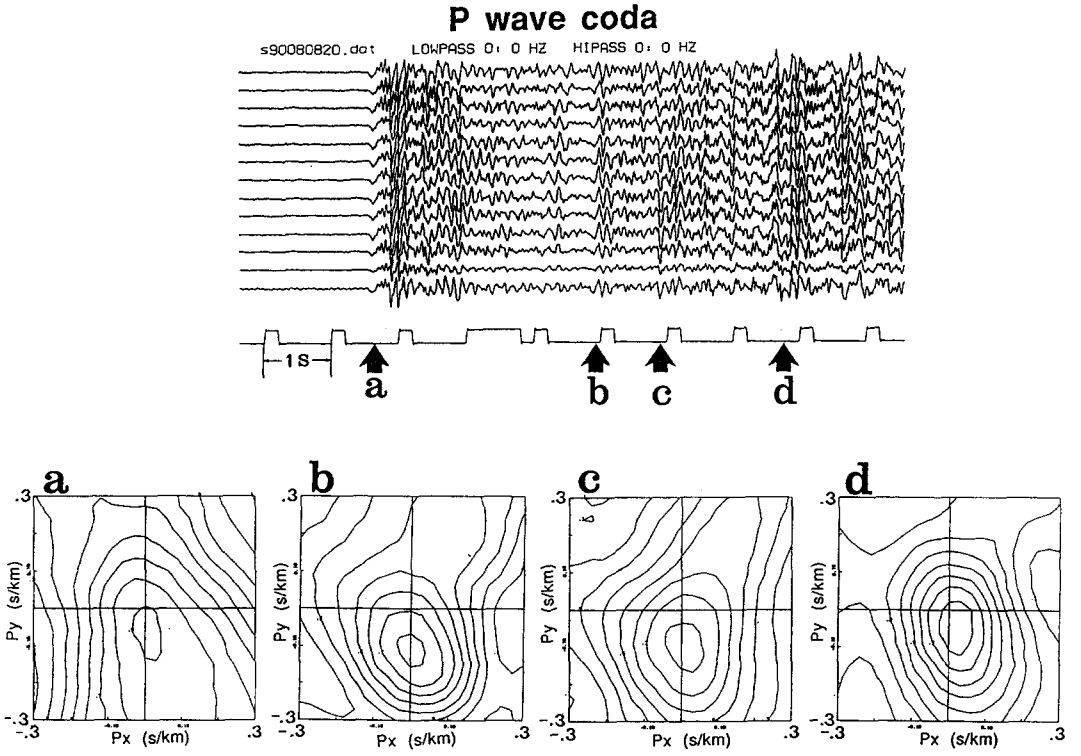

Fig. 4. Contour plots of semblance in the slowness vector plane for the Z-component of the direct P-wave and the P-coda. The diagrams a, b, c and d are for time windows of 0.1 s duration. The hypocenter of this event is located at 35.774°N, 140.181°E, and the depth of 111.5 km.

the energy of each trace within the same time window. Fig. 4 shows the semblance plots in the slowness vector plane for the Z-component in the time window of 0.1 s for the direct P-wave and the different clear phases in the P-coda. The hypocenter of this event is located at 35.774°N, 140.181°E, and the depth of 111.5 km. The time window of 0.1 s is almost the same as the dominant seismic wave period in this case. The position of the semblance maximum in the plot indicates the arrival azimuth and the horizontal slowness of the most dominant wave energy in the time window of the analysis. Fig. 4a shows that the arrival azimuth of the direct P-wave almost corresponds to the epicentral direction. It is, thus, understood that the semblance technique works well. Fig. 4b-d shows the results for different clear phases in the P-coda. It is noted that the arrival directions for these phases are almost the same as that of the direct P-wave.

3. Coda wave decomposition

3.1. Vertical component

In order to see the arrival direction of wave energy dominant in coda waves, we made plots of time series of the arrival azimuth, the slowness and the semblance value of the wave energy showing the maximum semblance in each time window. Fig. 5 shows a typical example of the plot of coda arrival azimuth (a), the slowness (b) and the semblance value (c) against the lapse time for the vertical component. This result is for the event shown in Fig. 3. The time window for the semblance calculation is about 0.2 s. It is understood that the P-coda of the vertical component is stably dominated by wave energy propagating parallel to the direct P-wave. The slowness of the energy is also almost the same as the direct P. Thus, the dominant energy in the P-coda vertical component is probably P-wave type energy. It is noted that the semblance values are generally larger than 0.5 in the P-coda. The semblance value can be interpreted as the ratio of energy along the proposed propagation direction to the total observed seismic energy (Neidell and Taner, 1971). It is, thus, found that more than half of the total seismic energy is propagated in the hypocentral direction.

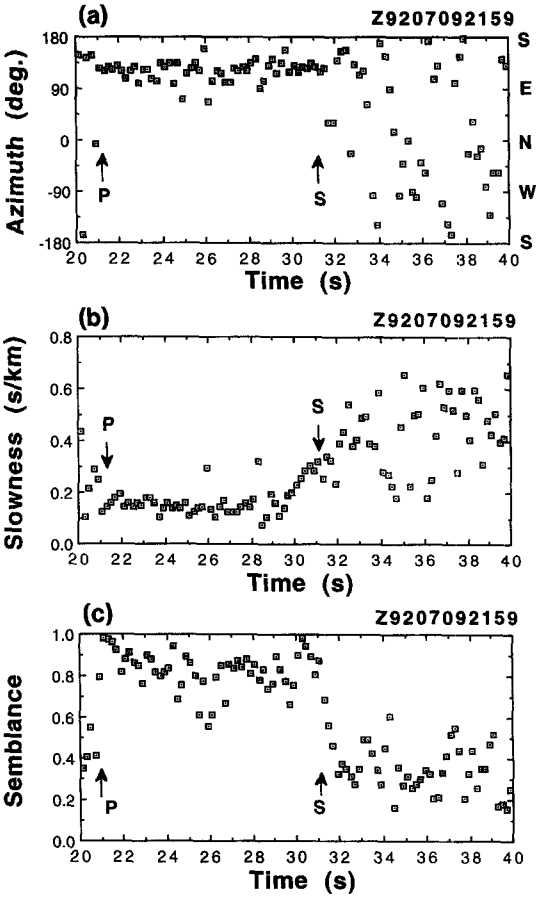

Fig. 5. Results of coda wave decomposition for the Z-component by means of the semblance technique for the event shown in Fig. 3. (a) Time series of arrival azimuths of wave energy dominant in the coda wave. (b) Time series of slowness values of dominant wave energy. (c) Time series of semblance values of dominant wave energy. The semblance value is the ratio of energy along a propagation direction indicated in the diagrams (a) and (b) to the total seismic energy.

The S-coda is very different from the P-coda. We can see that the S-coda is composed of wave energy arriving from random directions in Fig. 5. The slownesses have also various values generally larger than those in the P-coda. Further, the semblance values are relatively low, indicating that only a small portion of the total seismic energy is propagating from the direction determined from the maximum semblance value. These results indicate that the S-coda can be interpreted to be composed of wave energy propagated from random directions.

The above-mentioned properties of the vertical component are common especially for the shallow events whose epicentral distance is relatively small. This is because the scatter of the arrival azimuth does not represent the true scatter of the propagation direction but the apparent one. The arrival azimuth is defined as the projection of the propagation direction into the horizontal plane. Thus, the arrival azimuths of the coda waves are apparently more scattered for the event whose ray incidence angles of coda waves are small even though the true scatter of propagation directions is small. This means that when the epicentral distance becomes large, the scatter of the arrival azimuth of coda waves becomes large.

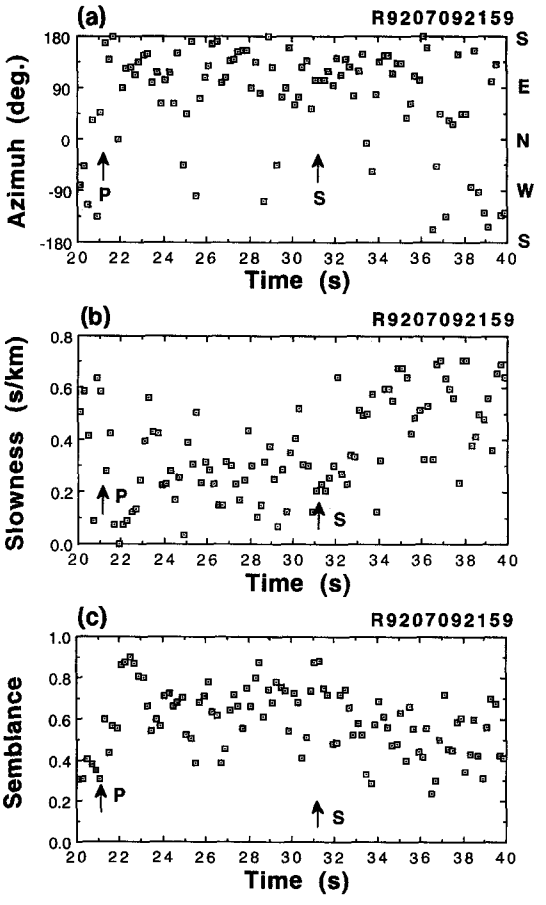

Fig. 6. Results of coda wave decomposition for *R*-component. See Fig. 5 for full explanations.

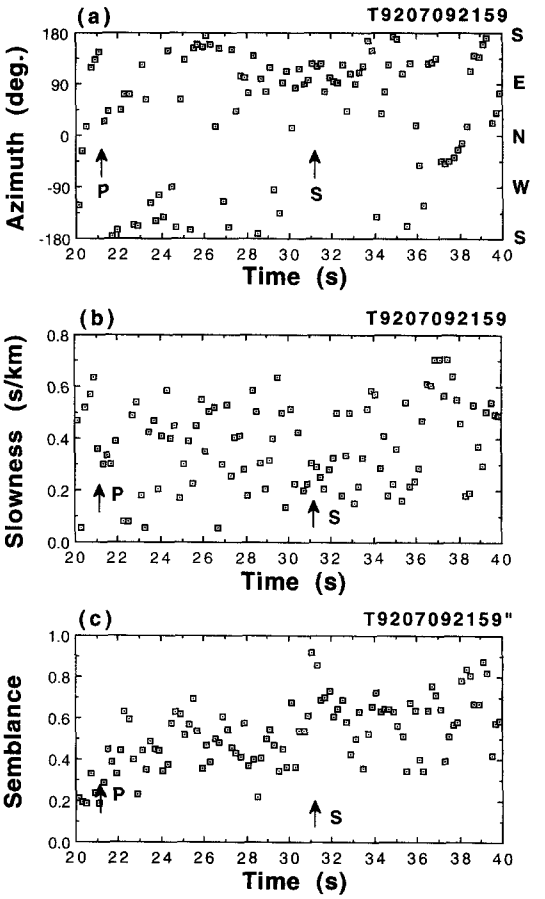

Fig. 7. Results of coda wave decomposition for *T*-component. See Fig. 5 for full explanations.

3.2. Horizontal components

Figs. 6 and 7 show the results of coda decomposition for the radial and transverse component, respectively. Compared with the vertical component, the P-coda is composed of wave energy with random propagation directions for both the horizontal components. It is noted that the semblance values of the radial component are larger than those of transverse components in the P-coda. In the S-coda, the propagation directions of the horizontal components are also random, while the semblance values are larger than those of the vertical component. The values gradually lessen from the high value of the direct S-wave.

4. Crustal heterogeneity model

Heterogeneity models can be divided generally into two categories: One is the layered structure model, the other is the laterally heterogeneous one. In these models, the coda waves are considered to be composed of refractions or reflections from the layered structure and of scattered waves from the lateral heterogeneity, respectively. In order to explain the observed characteristics of P- and S-coda, we propose a unified model where the heterogeneities are composed of a dominant layered structure with relatively weak lateral heterogeneity. Let us consider the effects of the layered structure and of the lateral heterogeneity on the coda waves, respectively, as shown in Fig. 8. Fig. 8a and b shows the effects of the layered structure and of the lateral heterogeneity, respectively, on the P-coda. In the case of Fig. 8a, the refractions at the interfaces of layered structure such as S to P or P to S are dominant in the P-coda. It is noted that the propagation directions of these phases are sub-parallel to the direct P-wave. Therefore, these types of phases can be candidates for the P-coda. Regarding the amplitude of P-coda, the conversion coefficient at the interface should be evaluated. Although the conversion coefficients are theoretically a complicated functions of incidence angles at the interface, the coefficients are roughly of an order $\Delta V_z/V$, where ΔV_z and V are the velocity jump at the boundary and the mean velocity of the structure, except at the critical incidence angle (Aki and Richards, 1980). Further, the mean S-wave energy radiated from earthquake sources is about 20 times as large as the P-wave energy. Therefore, the amplitude of the S–P converted phase at the interface is roughly the same as that of the direct P-wave amplitude, when $\Delta V_z/V$ is of the order of 10%. Compared to that, the amplitude of the P–S converted phase is probably much smaller. On the other hand, the propagation directions of scattered waves due to the lateral heterogeneity are random, as shown in Fig. 8b. Therefore, the effect of lateral heterogeneity has to be smaller than that of the layered structure. The velocity fluctuation $\Delta V_h/V$ in lateral heterogeneity should to be less than $\Delta V_z/V$ to comply with this requirement.

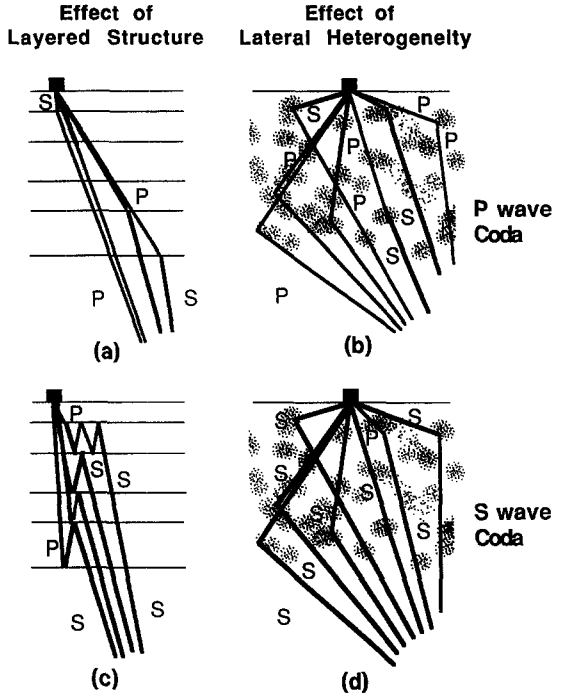

Fig. 8. Models of P- and S-coda excitation due to a layered structure and lateral heterogeneity. (a) Effects of the layered structure in the P-coda. (b) Effects of lateral heterogeneity in the P-coda. From the observational result, it is inferred that the effect of (a) is stronger than that of (b). (c) Effects of the layered structure in the S-coda. (d) Effects of lateral heterogeneity in the S-coda. The effect of (d) is stronger than (c).

The S-coda is considered in the same manner. Fig. 8c and d explains the effect of both types of heterogeneities for the S-coda. Multiple reflections such as S–S–S or S–P–P and so on in the layered structure of Fig. 8c can compose the S-coda, while the single reflection obviously cannot compose the S-coda. Thus, the amplitudes of such multiple reflected phases are of the order $(\Delta V_z/V)^2$ or less than that. Regarding the lateral heterogeneity in Fig. 8d, the single scattered wave such as S–S can contribute to the S-coda. In this case, the propagation direction becomes random. The amplitude of such scattered wave is also of the order $\Delta V_h/V$. Since the results of the array observation show that the propagation directions are random in the S-coda, the effect of the lateral heterogeneity should be larger than the effect of the layered structure so that $\Delta V_h/V > (\Delta V_z/V)^2$.

Summarizing the foregoing discussions, our observations introduce constraints about the velocity fluctuation in the heterogeneities. The velocity fluc-

tuation in the horizontal direction is larger than the square of that in the vertical direction, although the horizontal fluctuation is smaller than that of the vertical one, as shown in the following inequality:

$$(\Delta V_z/V)^2 < \Delta V_h/V < \Delta V_z/V.$$

5. Discussion

Sato (1984) calculates the excitation of coda waves due to all the scattered phases such as P–P, P–S, S–P, S–S in an isotropic heterogeneity model. He shows that S–P converted waves are dominant in the P-coda of the vertical component in the isotropic heterogeneity. In order to examine whether his isotropic heterogeneity model can explain our present observations of the P-coda, we calculate the range of scatters of the arrival azimuth for the S–P converted phase due to the isotropic heterogeneity. The range between the two bold curves in Fig. 9 is the theoretical one for the incidence angle is $\pi/2$. It is noted that the theoretical curves show the minimum range, because the range of the azimuth become larger for the incidence angle less than $\pi/2$. Therefore, the range of the actual data should be larger than that of the theoretical curves even though the isotropic heterogeneity mode can be applicable to the real structure. Considering the above discussion, it is remarkable in Fig. 9 that the actual data for the

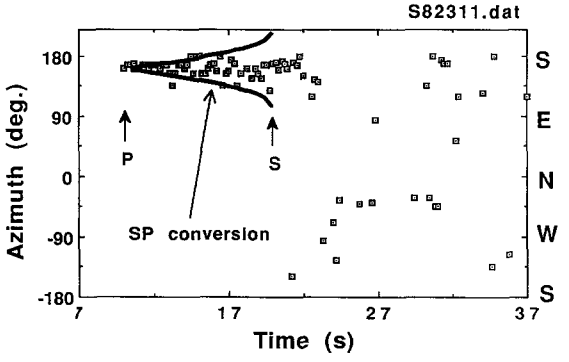

Fig. 9. Comparison between the actual data of arrival azimuths and a theoretical range of propagation azimuth of S–P converted phase due to the isotropic heterogeneity model of Sato (1984). The actual data is for the event whose hypocenter is located at 35.395°N, 140.443°E, and the depth of depth 34.8 km.

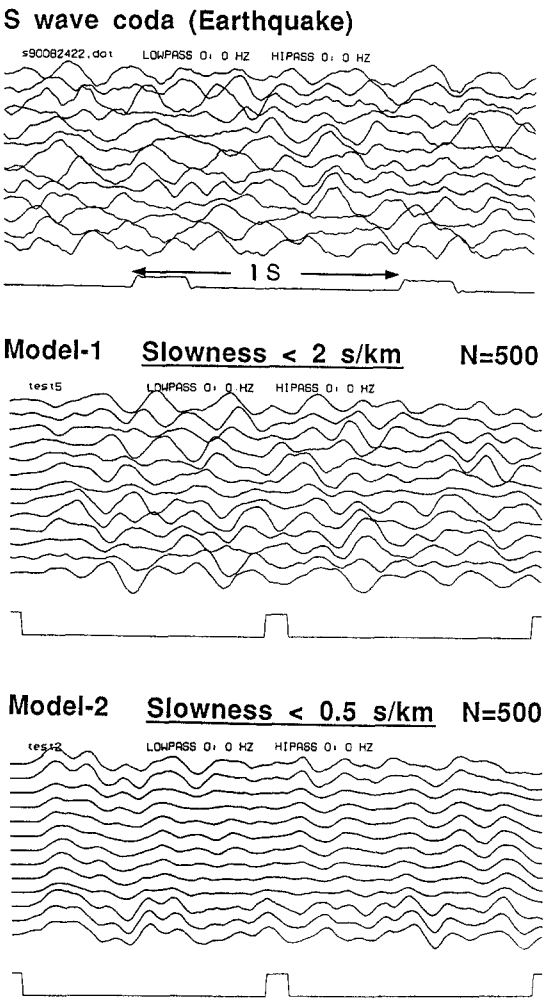

Fig. 10. Comparison between actual S-coda waveforms and synthetic waveforms. Synthetics of Model-1 include the horizontal propagation of S-wave or surface waves. Those of Model-2 are composed by wave energy with relatively small slownesses.

event, whose hypocenter is located at 35.395°N, 140.443°E, and the depth of depth 34.8 km, are lying in a smaller range than the theoretical one. This remarkable feature obviously holds true also for the event shown in Fig. 5. These results indicate that the isotropic model is not applicable. We thus conclude that the layered structure is necessary to explain our observations.

The semblance technique does not seem to work for the S-coda, because the semblance values are too small in the S-coda. In order to evaluate the range of slowness of the S-coda, we calculate synthetic wave-

forms simply by summing 500 wavelets of a sine shape with random phases and random slownesses. With reference to the velocity structure shown in Table 1, we calculate two synthetic array waveforms composed by 500 random phases with slownesses less than 2 s/km and less than 0.5 s/km. The first model represent the coda wave including the horizontal propagation of S-wave or surface waves: the second one does not include such a large horizontal slowness. Fig. 10 shows the actual data of the S-coda and the synthetics. The synthetic waveforms of Model-1 are similar to the actual data in contrast to Model-2. Therefore, it is very likely that the S-coda include the horizontally propagating S-waves or surface waves.

Our results of P- and S-coda in Tsukuba are found to be almost the same as those in Oshima volcano and other locations (Kuwahara et al., 1990; Jepsen and Kennett, 1990; Wagner and Owens, 1993). As mentioned in the introduction, Kuwahara et al. (1990) proposed a model of P-coda generation due to the trapped waves in a low velocity zone of subducting oceanic crust. However, it is obvious that this interpretation is not unique, because the crustal heterogeneity model proposed in this study can be also applicable to the Oshima volcano.

Although the vertical components are, so far, discussed in detail, the horizontal components are also consistent with the present model. Because in general the ray direction of S–P converted phases due to the layered structure has a small incidence angle, the S–P phases are mainly observed in the P-coda of the vertical component. This means that the effect of the layered structure is small in the radial component and that the effect does not appear in the *T*-component. The horizontal components are affected mainly by the lateral heterogeneity. Thus, the propagation direction is expected to be random from the discussed heterogeneity model, and this is consistent with the observations.

6. Conclusion

The analysis of small-aperture seismic array data reveals the compositions of P- and S-coda. It is found that the propagation directions of the P-coda energy of the vertical component are sub-parallel to that of the direct P-wave. However, the P-coda of the horizontal components shows random directions. The S-codas of all the three components also show random directions. These features indicate that the converted S to P-waves at horizontal boundaries of the structure are dominant in the P-coda of the vertical component, while the P-coda of the horizontal components and the S-coda consist of scattered waves from lateral heterogeneities. This interpretation leads to the model of crustal heterogeneity in which the velocity fluctuation in the horizontal direction is larger than the square of that in the vertical one, although the horizontal fluctuation is smaller than the vertical one.

Acknowledgements

We thank the National Research Institute for Earth Science and Disaster Prevention of Japan for providing the hypocenter data. We are grateful to the two anonymous reviewers for their helpful comments and suggestions.

References

Aki, K., 1959. Correlational study of near earthquake waves. Bull. Earthq. Res. Inst. 36, 207–232.

Aki, K., 1969. Analysis of the seismic coda of local earthquakes as scattered waves. J. Geophys. Res. 74, 615–631.

Aki, K., Chouet, B., 1975. Origin of coda waves: source, attenuation and scattering effects. J. Geophys. Res. 80, 3322–3342.

Aki, K., Richards, P.G., 1980. Quantitative Seismology, W.H. Freeman, San Francisco, 932 pp.

Campillo, M., Paul, A., 1992. Influence of the lower crustal structure on the early coda of regional seismograms. J. Geophys. Res. 97, 3405–3416.

Dainty, A.M., Toksoz, M.N., 1990. Array analysis of seismic scattering. Bull. Seism. Soc. Am. 80, 2242–2260.

Fuchs, K., Bonjer, K.-P., Gajewski, D., Lushen, E., Prodehl, C., Sandmeier, K.-J., Wenzel, F., Wilhelm, H., 1987. Crustal evolution of the Rhinegraben area: 1. Exploring the lower crust in the Rhinergraben rift by unified geophysical experiments. Tectonophysics 141, 261–275.

Ishida, M., 1992. Geometry and relative motion of the Philippine Sea plate and Pacific plate beneath the Kanto-Tokai district, Japan. J. Geophys. Res. 97, 489–513.

Jepsen, D.C., Kennett, B.L.N., 1990. Three-component analysis of regional seismogram. Bull. Seism. Soc. Am. 80, 202–2052.

Kennett, B.L.N., 1987. Observational and theoretical constraints on crustal and upper mantle heterogeneity. Phys. Earth Planet. Interiors 47, 319–337.

King, D.W., Mereu, R.F., Muirhead, K.J., 1973. The measurement of apparent velocity and azimuth using adaptive processing techniques on data from the Warramunga seismic array. Geophys. J. R. Astr. Soc. 35, 137–167.

Kinoshita, S., 1990. The earthquake response characteristics of a thick sedimentary layer estimated by means of the deep-borehole observation. Rep. National Res. Center Disaster Prev. 38, 25–145.

Kuwahara, Y., Ito, H., Shinohara, M., Kawakatsu, H., 1990. Small-array observation of seismic coda waves in Izu-Oshima —Analysis of coda waves from artificial explosions and from a natural intermediate-depth earthquake. J. Seismo. Soc. Jpn. (Zisin) 43, 359–371, in Japanese with English abstract.

Neidell, N.S., Tanner, M.T., 1971. Semblance and other coherency measures of multichannel data. Geophysics 36, 483–497.

Sato, H., 1984. Attenuation and envelope formation of three component seismograms of small local earthquakes in randomly inhomogeneous lithosphere. J. Geophys. Res. 89, 1221–1241.

Wagner, G.S., Owens, T.J., 1993. Broadband bearing-time records of the three-component seismic array data and their application to the study of local earthquake coda. Geophys. Res. Lett. 20, 1823–1860.